

Manuscript Number:

Title: Assessing the ageing process of cation exchange membranes in bioelectrochemical systems

Article Type: Full Length Article

Section/Category: Electrolysis / Electrolyzers

Keywords: Bioelectrochemical system; Cation exchange membranes; Ageing of membranes; Microbial electrolysis cell.

Corresponding Author: Miss María Isabel San Martín,

Corresponding Author's Institution: Universidad de León

First Author: María Isabel San Martín

Order of Authors: María Isabel San Martín; Francisco Javier Carmona; Pedro Prádanos; Antonio Morán, Professor; Adrián Escapa

Abstract: Bioelectrochemical systems (BES) encompass a group of biobased technologies capable of directly converting organic matter into electricity. In these systems, which are derived from conventional electrochemical technologies, the ion exchange membrane represents a key element because of its influence on the economic feasibility and on the performance of BES. This study examines the impact of long-term operation of a BES on the mechanical, chemical and electrochemical properties of five different kind of cation exchange membranes (Nafion-117, CMI-7001, Zirfon UTP 500, FKE and FKB) through several techniques: (i) scanning electron microscopy (SEM) and atomic force microscopy (AFM) to assess the changes on the membranes surface, (ii) thermogravimetric analysis (TGA) to evaluate the structural stability of the membranes, and (iii) ion exchange capacity (IEC) to monitor any change in their electrochemical properties. Results confirmed that there is not an ideal membrane for BES. While Nafion and CMI-7000 exhibited the strongest chemical structure, they also underwent the highest fouling as revealed by a fast increase in surface roughness.

1 Assessing the ageing process of cation 2 exchange membranes in bioelectrochemical 3 systems

4 **M. Isabel San-Martín¹, Francisco Javier Carmona², Pedro Prádanos³, Antonio Morán¹,**
5 **Adrián Escapa^{1,4,*}.**

6
7 ¹ Chemical and Environmental Bioprocess Engineering Group, Natural Resources Institute
8 (IRENA), Universidad de León, Avda. de Portugal 41, 24009, León, Spain.

9 ² Dpto. de Física Aplicada. Escuela Politécnica, Universidad de Extremadura, 10004 Cáceres,
10 Spain.

11 ³ Grupo de Superficies y Materiales Porosos, Dpto. Física Aplicada, Facultad de Ciencias,
12 Universidad de Valladolid, 47071, Valladolid, Spain.

13 ⁴ Department of Electrical Engineering and Automatic Systems, Universidad de León, Campus de
14 Vegazana s/n, 24071 León, Spain

15
16 * **Corresponding author:** adrian.escapa@unileon.es e-mail@e-mail.com; Tel.: +34 987295394

17

18 **Abstract:** Bioelectrochemical systems (BES) encompass a group of biobased
19 technologies capable of directly converting organic matter into electricity. In these systems,
20 which are derived from conventional electrochemical technologies, the ion exchange
21 membrane represents a key element because of its influence on the economic feasibility
22 and on the performance of BES. This study examines the impact of long-term operation of
23 a BES on the mechanical, chemical and electrochemical properties of five different kind of
24 cation exchange membranes (Nafion-117, CMI-7001, Zirfon UTP 500, FKE and FKB)
25 through several techniques: (i) scanning electron microscopy (SEM) and atomic force
26 microscopy (AFM) to assess the changes on the membranes surface, (ii)
27 thermogravimetric analysis (TGA) to evaluate the structural stability of the membranes, and
28 (iii) ion exchange capacity (IEC) to monitor any change in their electrochemical properties.
29 Results confirmed that there is not an ideal membrane for BES. While Nafion and
30 CMI-7000 exhibited the strongest chemical structure, they also underwent the highest
31 fouling as revealed by a fast increase in surface roughness.

32 **Keywords:** Bioelectrochemical system; Cation exchange membranes; Ageing of
33 membranes; Microbial electrolysis cell.

34 **Highlights**

- 35 • No significant fouling, breakings or deformities in membrane surfaces were
36 observed.
 - 37 • Nafion and CMI showed the most robust chemical structure and roughness
38 increase.
 - 39 • The ion exchange capacity showed a moderate decay in all membranes.
 - 40 • After the four-month membrane operation, the current density kept almost
41 constant ($\sim 1 \text{ A}\cdot\text{m}^{-2}$).
42
-

43 **1. Introduction**

44 For the last 15 years, bioelectrochemical systems (BES) have experienced an
45 intense phase of research and development, proving to be a versatile group of
46 technologies with a wide range of potential applications (e.g.: energy recovery from
47 organic matter, chemical production from carbon dioxide, nutrient recovery from
48 waste streams, etc.) [1]. BES are also capable of utilising a broad range of organic
49 and inorganic substrates [2] which gives them a great operational flexibility. Despite
50 that, and despite the numerous scale-up endeavours reported in the literature [3],
51 BES are far from being a mature technology [4]. The still low current densities,
52 relatively large capital cost and the difficulties associated with energy
53 harvesting/management are often reported as major challenges in their way towards
54 practical application.

55 The ion exchange membrane (IEM), which is a core element in BESs, has a
56 significant impact on both the performance [5] (e.g.: coulombic efficiencies and
57 internal electrical resistance) and the capital costs [4], being responsible for up to
58 40% of the overall cost of BES [6]. Thus, it is not surprising that, in an effort to
59 improve the commercial perspectives of BES, many researcher groups have come
60 up with alternative designs that completely dispense with the membrane. Although
61 many of them have proved to be successful in several fields of application such as
62 organic and inorganic contamination removal [7,8] or energy production [9], the IEM
63 becomes a critical element when the aim is to optimize energy efficiency (by
64 avoiding oxygen and hydrogen crossover [4,6]) or accomplish processes of
65 industrial interest (nutrients recovery, microbial electrosynthesis or seawater
66 desalination [10][11][12]). The application of several types of IEM such as anion
67 exchange membranes (AEM), cation exchange membranes (CEM), microfiltration
68 membrane, bipolar membrane and ultrafiltration membranes to BES has been

69 extensively covered in the literature [13]. Nafion has remained the most popular
70 because of its good mechanical stability and high proton selectivity [14], although its
71 high price has motivated the search for other cheaper alternatives [11], such as
72 Fumasep, Ultrex, Zirfon or Hyflon.

73 Ideally, a membrane apt for BES use should have low electrical resistance (to
74 facilitate the ion transport), should prevent gas and substrates diffusion, have a high
75 biofouling resistance and at a relatively with low-cost [15]. Membrane degradation,
76 commonly known as ‘membrane ageing’, is another important aspect as it is directly
77 related to their durability. Membrane ageing is usually characterised in terms of
78 physical, chemical and electrochemical stability and to this end, a vast array of
79 methods is available including microscopy, impedance spectroscopy or titration
80 technics. Previous studies have made use of these techniques to investigate the
81 ageing of individual membranes [16], but there is a lack of knowledge on how these
82 membranes compare in terms of their ageing patterns a stability. In this study, we aim
83 at filling this gap by assessing how the mechanical, chemical and electrochemical
84 properties of five commercially available cation exchange membranes develop
85 during four months of continuous operation within the environment of a microbial
86 electrolysis cell (MEC). All the membranes were subjected to identical operational
87 conditions by being fitted within the same MEC reactor. Membranes samples were
88 collected on a monthly basis. Scanning electron microscopy (SEM) and atomic
89 force microscopy (AFM) were used to assess the changes on the membranes
90 surface; thermogravimetric analysis (TGA) to evaluate the structural stability of the
91 membranes, and ion exchange capacity (IEC) to monitor any change in their
92 electrochemical properties.

93 **2. Materials and Methods**

94 *2.1. Microbial electrolysis cell design and operation*

95 This work assesses the ageing process of five commercially available CEM (see
96 section 2.2 for a complete description of them). To make sure that all membranes
97 were subjected to the same operational conditions (i.e.: same pH, temperature,
98 hydraulic retention time, etc) they were arranged within the same MEC reactor by
99 using the frame shown in Figure 1. This frame consisted of two identical
100 methacrylate plates with 30 windows (30 mm x 12 mm) opened in the plates to
101 accommodate the membranes samples (6 for each type of CEM tested). The two

102 plates were joined by small screws to facilitate the sampling process which was
103 carried out on a monthly basis (see section 2.2).

104 The anodic and the cathodic chambers were constructed with methacrylate
105 plates too and were separated by the frame above described. Each chamber
106 retained 230 mL of liquid and had a headspace of 20 mL. The anode was made of a
107 5 mm-thick graphite felt (Sigratherm®, Germany), and the cathode consisted of a
108 stainless steel mesh, both measuring 24.5 cm x 9.5 cm. The carbon felt was
109 pre-treated with a method listed elsewhere [17] and the stainless steel was cleaned
110 with distilled water. A titanium wire was used as current collector to connect the
111 electrodes to a power supply PS2000B (Elektro-Automatik, Germany). The applied
112 voltage was set at 1 V between anode and cathode and the electrical current was
113 recorded every 10 minutes across an 8 Ω resistor by means of a 2700 Keithley
114 multimeter (Keithley Instruments, USA).

115 The anode chamber was inoculated with a mixture activated sludge and effluent
116 from another MEC operated for 4 months. The anolyte stock solution was composed
117 0.55 g·L⁻¹ sodium acetate, 6 g·L⁻¹ K₂HPO₄, 3 g·L⁻¹ KH₂PO₄, 1.5 g·L⁻¹ NH₄Cl, 1 g·L⁻¹
118 NaHCO₃, 0.5 g·L⁻¹ NaCl, 0.2 mg·L⁻¹ CaCl₂, 0.15 g·L⁻¹ MgSO₄·7H₂O and 1 mL·L⁻¹ of
119 a mixed trace element solution and vitamins [18]. The catholyte stock solution
120 consisted of a 0.1 M phosphate buffer. Both were sparged with nitrogen gas for 20
121 minutes to ensure anaerobic conditions and stored at 4°C until use. Anolyte and
122 catholyte were feed in continuous mode by mean of two peristaltic pumps at a flow
123 rate of 30 mL·h⁻¹, thus providing a 7 h retention time.

124

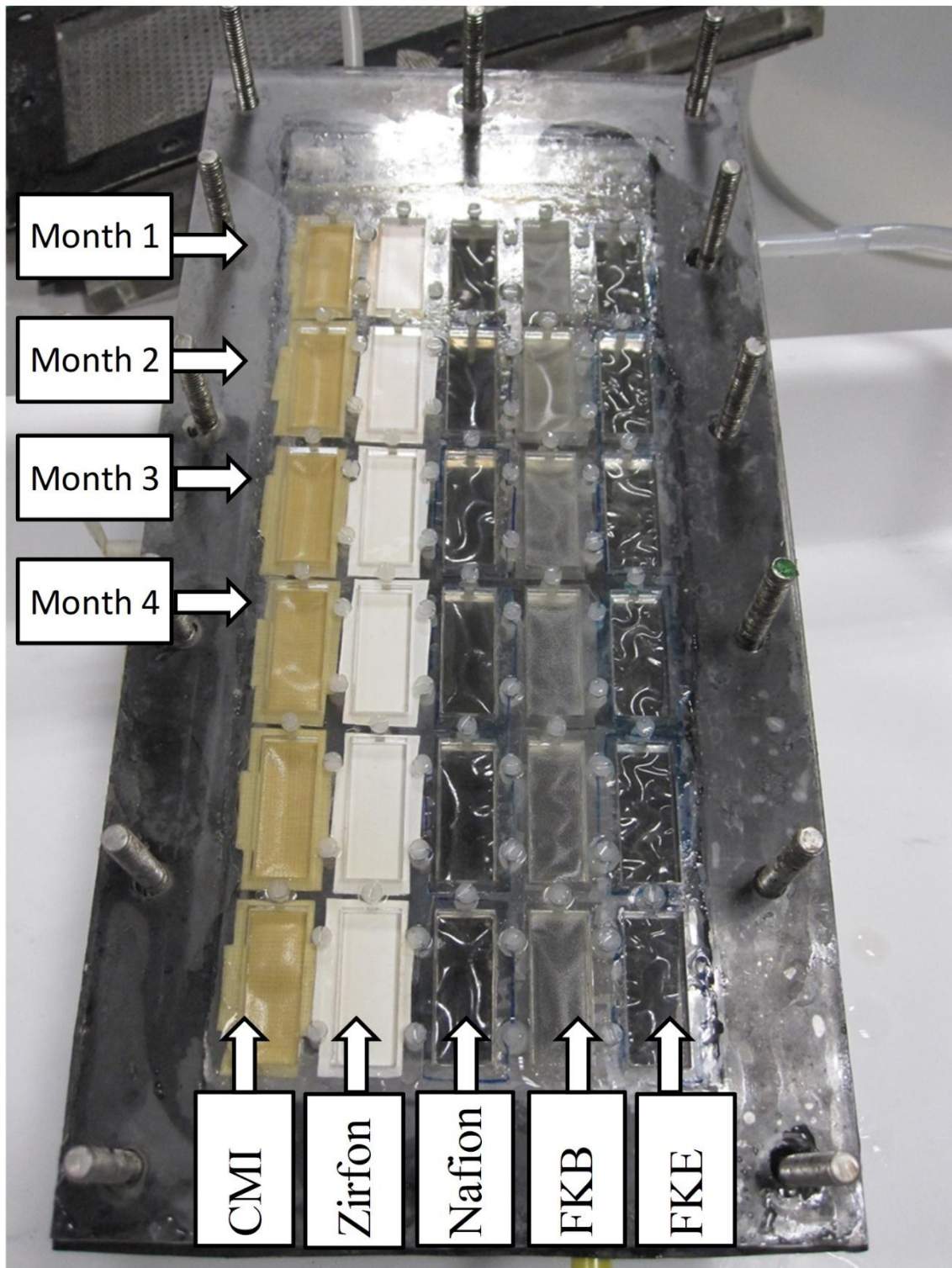


Figure 1. The methacrylate frame housing the 6x5 CEM membrane's samples

125
126

127 *2.2. Membranes and membranes characterisation*

128 Five commercially available CEM were used: Nafion 117 (DuPont, USA),
 129 CMI-7000 (Membranes International, USA), Zirfon Perl UTP 500 (Agfa, Belgium),
 130 Fumasep FKE and FKB (Fumatech, Germany). Table 1 shows some of their
 131 characteristics as provided by the manufacturer. After being placed in the frame

132 (Figure 1), the 5x6 membrane samples were soaked in demineralised water for at
 133 least 24 h.

Table 1. Physical and chemical properties of the cation exchange membranes used in this research

Property	Units	FKE	FKB	Nafion 117	Zirfon UTP 500	CMI-70 00
Selectivity	%	> 0.98	> 0.98	-	-	> 0.97
Electric resistance	$\Omega \cdot \text{cm}^2$	< 3	< 4	1.5	< 0.3	< 30
Stability	pH	1-14	1-14	-	6 M KOH	1-10
Thickness	mm	0.05-0.07	0.08-0.1	0.18	0.5	0.45
Ion exchange capacity	meq/g	> 1	0.9-1.0	0.95-1.01	-	1.6
Cost	€/m ²	195	320	400	45	170

134 The ageing process of the five membranes was assessed on samples taken after 1,
 135 2, 3 and 4 months of operation (Figure 1). After sampling, a fresh membrane was
 136 placed in the vacant window, the MEC was reassembled and both chambers were
 137 purged with nitrogen gas. Although the initial plan for the experiment was to continue
 138 the sampling process for 6 months (hence the 6 samples for each type of membrane
 139 in the frame), it was stopped at month 4 because the ageing tended to stabilize after
 140 the first month of operation of the MEC. The ageing of the membranes was
 141 evaluated according to the observed changes in their (i) superficial morphology
 142 (analysed by scanning electron microscopy and atomic force microscopy), (ii)
 143 structural stability (measured by thermogravimetric analysis), (iii) number of fixed
 144 charges inside the cation exchange membrane (measured according to the ion
 145 exchange capacity) and (iv) electrical resistance (calculated by electrical impedance
 146 spectroscopy). All these techniques are described in the following sections.

147 2.3. Scanning electron microscopy (SEM)

148 A JSM-6480 LV (JEOL, Japan) scanning electron microscope was used. The
 149 samples were fixed in a 2.5% glutaraldehyde solution in phosphate buffered saline

150 (PBS) solution for 2 hours at 4° C. After drying the membranes with ethanol, they
151 were transferred into the chamber of a critical point dryer CPD 030 (Bal-Tec,
152 Germany). Subsequently, prior to observation of the microstructure by SEM, the
153 membranes were coated with a thin layer of gold in a sputter coater equipment EM
154 ACE200 (Leica Microsystems, Switzerland).

155 *2.4. Atomic force microscopy (AFM)*

156 A Nanoscope Multimode IIIa scanning probe microscope from Digital
157 Instruments (Veeco Metrology Inc., USA) was used, following the method described
158 elsewhere [19]. The calculated values of surface roughness were averaged over 5
159 different profiles for each membrane sample using a scanning area of 1×1 μm². The
160 AFM allows to monitor changes on the membrane surface and get a quantitative
161 measurement of roughness as Sq [20]. Sq refers to the root mean square roughness
162 and represents the statistical measure of the magnitude of the height distribution. It
163 was calculated according to Eq. 1:

$$S_q = \sqrt{\frac{1}{mn} \sum_{i=1}^m \sum_{j=1}^n Z^2(x_i, y_j)} , \quad (1)$$

164

165 where m and n are the number of the pixels in the x and y directions
166 respectively (512×512 in this case), and Z is the height of a pixel.

167 *2.5. Thermogravimetric analysis (TGA)*

168 The thermogravimetric analyses were carried out with a Thermogravimetric
169 Analyzer SDT Q600 (TA Instruments, USA), in a temperature range from 30 to 750
170 °C, at the constant rate heating of 10 °C·min⁻¹, under nitrogen saturated
171 environment.

172 *2.6. Ion exchange capacity (IEC)*

173 The ion exchange capacity was determined by acid-base titration. Initially the
174 membranes samples were immersed in distilled water and soaked in a large volume
175 of 1 M HCl solution for at least 24 hours (the solution was replaced three times to
176 complete the ion exchange). After that, they were washed again with distilled water
177 to remove the excess of HCl and soaked in a 2 M NaCl solution for at least 24 hours
178 to replace the protons by sodium ions (similary, the solution was replaced three

179 times to ensure a complete exchange). The different NaCl solutions were collected
180 and then titrated with 0.1 M NaOH. The ion exchange capacity titration of the
181 membrane was calculated as the ratio between the total charge (meq) and the dry
182 weight of the measured membrane (g).

183 **3. Results and discussion**

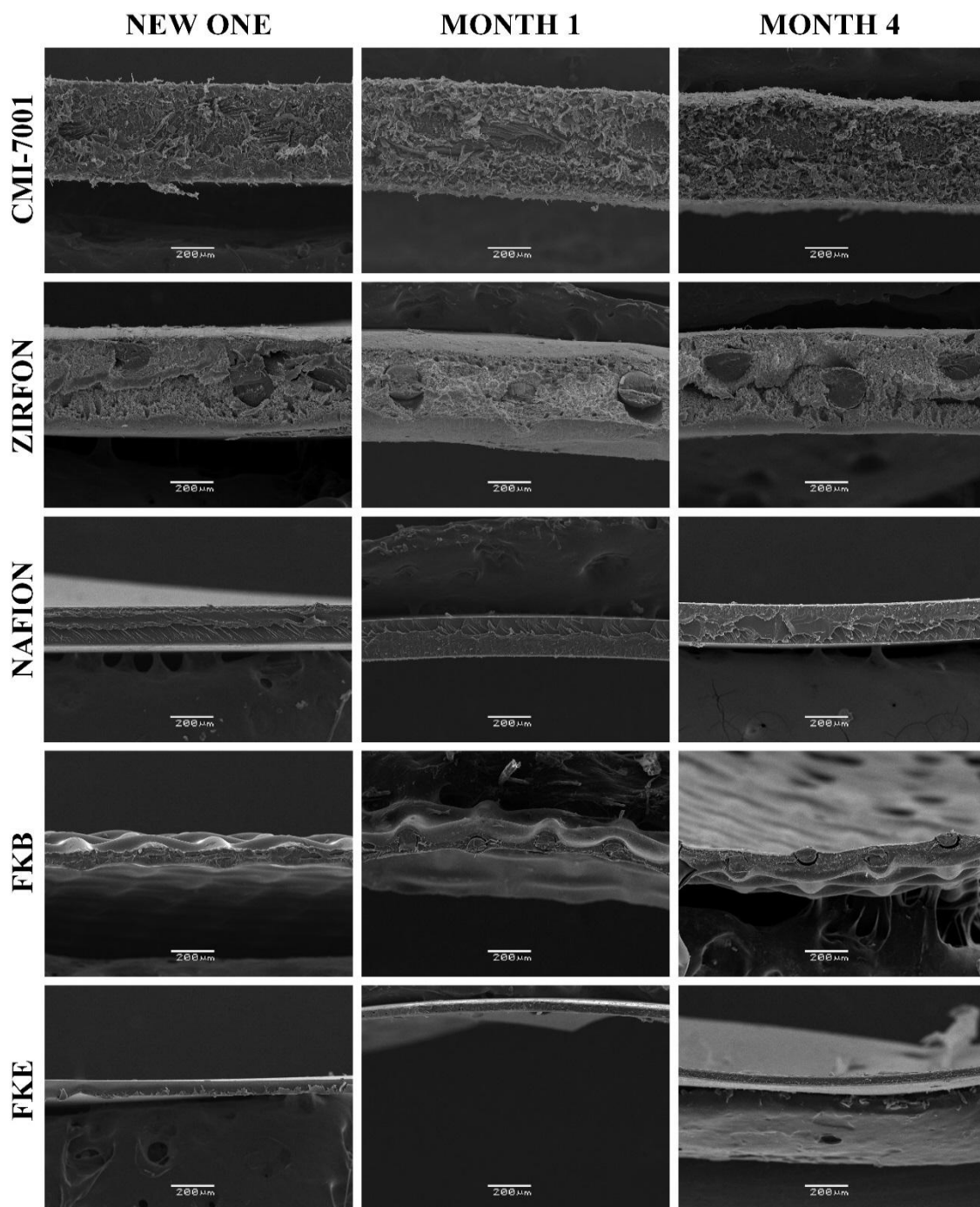
184 As described in section 2.2, the ageing of the five membranes considered in this
185 study was assessed according to modification in their surfaces, structural stability
186 and ionic exchange capacity. In the following paragraphs, these properties are
187 described and discussed in detail.

188 *3.1. Assessment of membrane surface modifications through SEM and AFM*

189 Cation exchange membranes are liable to undergo biological and chemical
190 fouling when operated in BESs [21]. The interest in tracking this phenomenon lays in
191 the fact that fouling represents a physical blockage to charge transport through the
192 membrane, which can result in a decay of current [22]. Although there is no specific
193 procedure to measure its formation rates, SEM can provide a qualitative estimation
194 of its physical extent [6]. As it can be observed in Figure 2, SEM analyses did not
195 reveal any visible difference between fresh (unused) membranes and those samples
196 taken after 1 and 4 months of operation. No biofouling was perceptible on either the
197 anode nor on the cathode side and no breakings or deformities in the internal
198 structure of the membranes were detected at a 90x magnification.

199 Still, these results need to be interpreted with caution precisely because of their
200 qualitative nature. The apparent lack of any of surface deterioration might be hiding
201 inorganic salts precipitations, biomass and extracellular polymers that are not easily
202 perceptible on the SEM images and that may be depositing on the membranes
203 surfaces. Here, monitoring the evolution of surface roughness through AFM
204 analyses and computed by the root mean square roughness (S_q , see section 2.4)
205 can provide an indirect and quantitative evidence of fouling (any change on S_q in
206 membranes exposed to bioreactors indicates that foulants are deposited [23]).
207 Figure 3 shows how S_q increases more visibly in CMI and Nafion membranes
208 (especially after the first month of operation). The Zirfon membrane, despite
209 displaying the highest surface roughness on the fresh sample (probably because of
210 the presence of ZrO_2), developed the least relative increase over the four months of

211 operation which might be indicative of low fouling. This is indeed a surprising result,
212 as membranes with high initial surface roughness tend to promote biofouling more
213 easily [24], which clearly contrasts with our results. The roughness of FKB and FKE
214 membranes increased progressively along the four months but always kept below
215 the other three membranes studied.
216

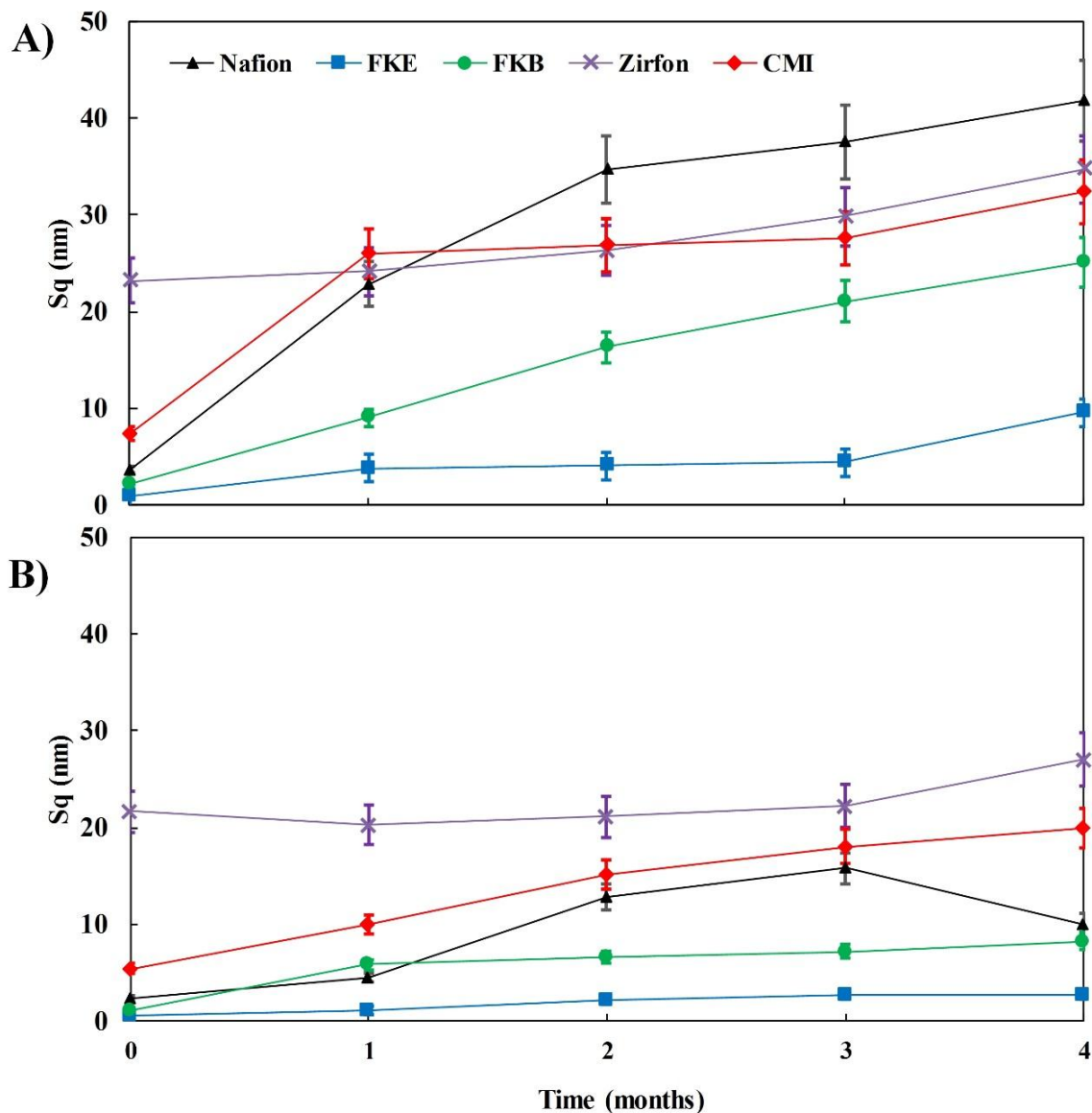


217
218
219

Figure 2. Cross-sectional SEM images of new membranes after 1 and 4 months of operation (90x magnification).

220 Figure 3 also shows a clear divergence in the evolution of Sq on both sides of the
221 membrane; while the anode side displayed a faster increase and a higher surface
222 roughness, the evolution of Sq on the cathode side was more moderate. This
223 difference can be explained by the higher salt concentration and the presence of
224 biomass on the anode side which could be promoting the fouling process.

225 Thus, on account of these results, when dealing with substrates with a high salts
226 content (e.g.: landfill leachate or seawater) or substrates with planktonic biomass or
227 complex organic compounds (eg.: wastewater, effluent from anaerobic digestion),
228 Zirfon, FKE and FKB membranes may be more advantageous than the CMI and the
229 Nafion.



230

231 **Figure 3.** Sq (nm) variation as a function of time on the side in contact with the anolyte (A)

232 and on the side in contact with the catholyte (B).

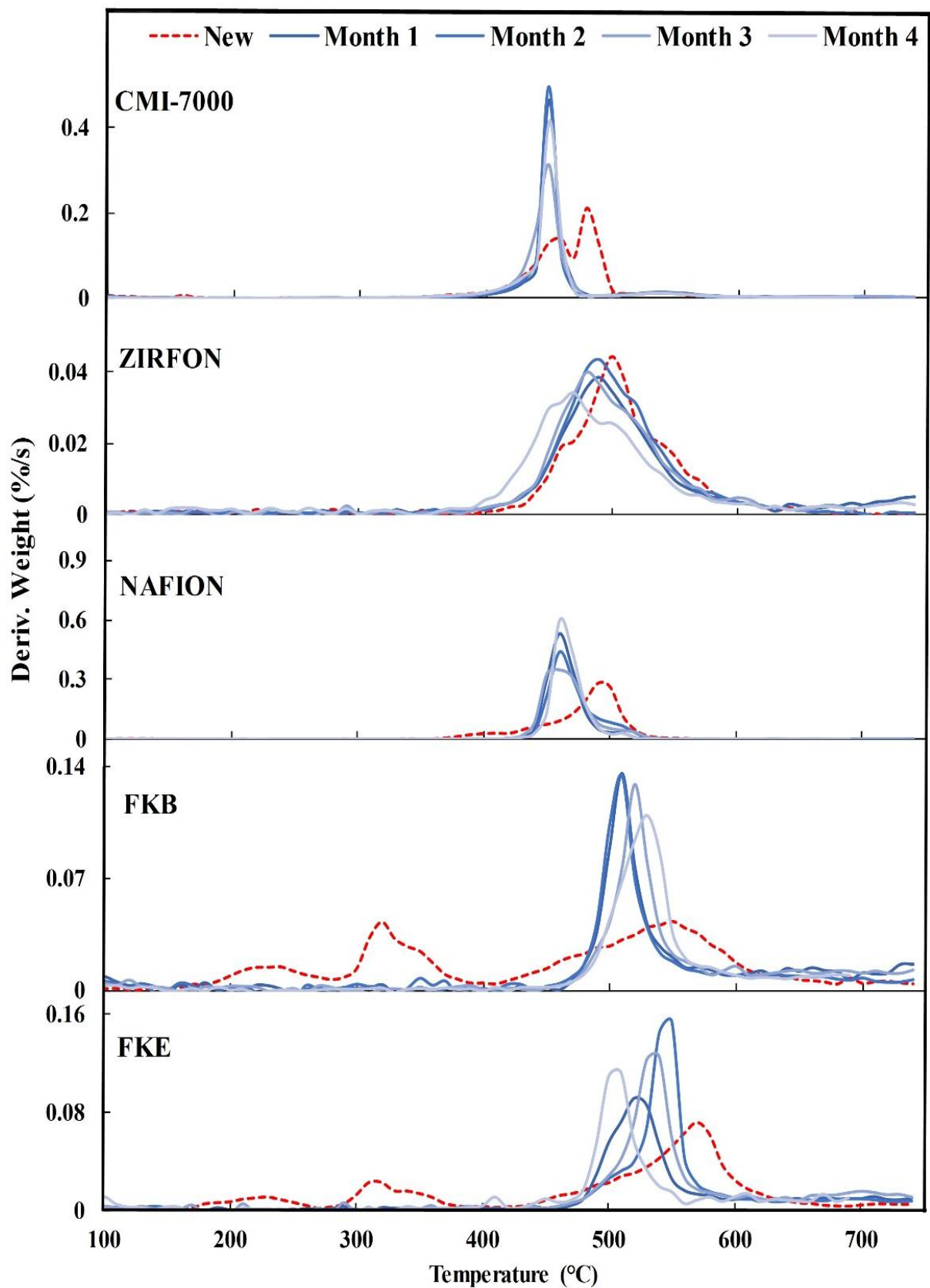
233 3.2. Assessment of membrane structural deterioration through TGA

234 As mentioned before, the lack of any visible deterioration in the membrane
235 structure, as observed in the SEM images (Figure 2), does not necessarily means
236 that the structural stability of the membrane remains unaffected. Indeed, the ageing
237 process can also be affecting the polymer matrix and the functional groups of the
238 membranes. Modifications in any of them were evaluated by monitoring the changes
239 in thermal stability of the samples (Figure 4).

240 The CMI-7000 consists of cross linked gel polystyrene with divinylbenzene and
241 sulphonic acid as the functional groups [25]. The peak that appears on the TGA
242 profiles between 400 °C and 490 °C (Figure 4A) is attributed to the decomposition of
243 the polystyrene chains together with $-\text{SO}_3\text{H}^-$ groups, while the peak above 500 °C
244 would most likely be ascribed to the decomposition of the residual solvent from the
245 manufacturing process that is not anchored to the matrix and lost with use. The TGA
246 profiles show a clear divergence between the new and the used membranes: the two
247 peaks that appear on the unused membrane merge into just one peak in used
248 membranes and get displaced towards low temperatures. Beyond this change, there
249 is no evidence of degradation along time, that is, the membrane structure remains
250 fairly stable after this first month of operation.

251 For the Zirfon membrane, which consists of a hydrophilic polyphenylene
252 sulphide fabric coated with a mixture of a polymer and zirconium oxide [26], the
253 degradation patten was more gradual and continued after the first month. However,
254 in this case it is difficult to establish a relation between the peaks that appear in the
255 TGA profile and the degradation of any of the compounds that integrate the
256 membrane because there is scant information about the characteristic of the Zirfon
257 membrane in the technical and scientific literature.

258



259 **Figure 4.** Thermogravimetric analysis of the membranes before (red dash line) and after 1,
 260 2, 3 and 4 months of operation (gradient of blue lines).
 261

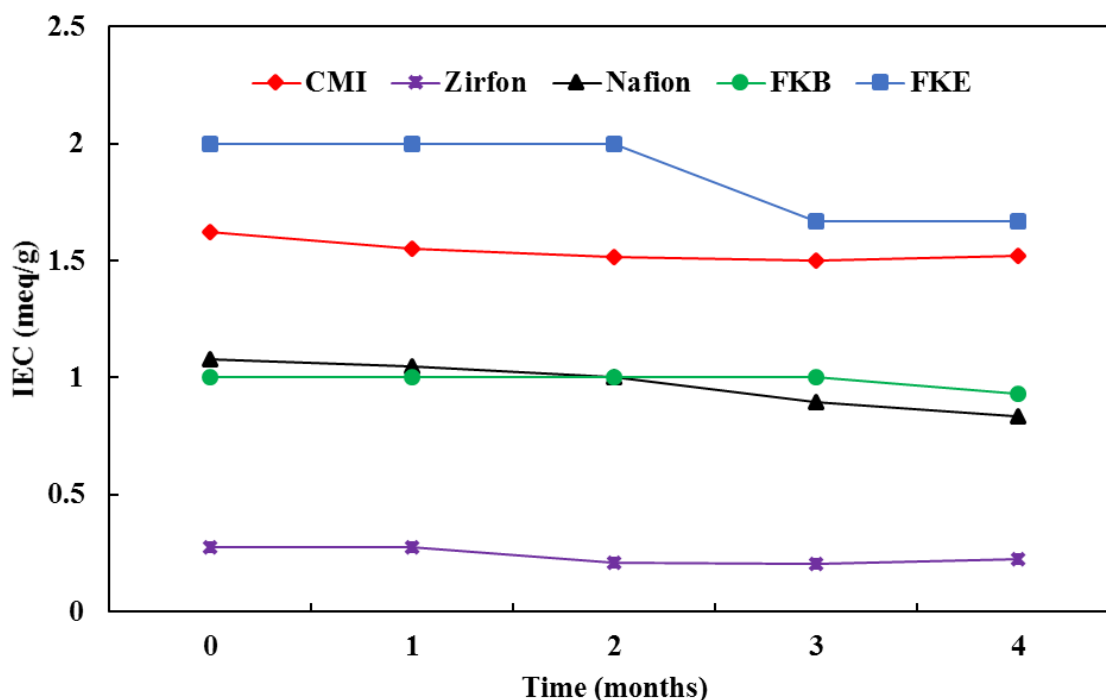
262 The Nafion membrane is a perfluorinated membrane made of carbon–fluorine
263 backbone chains and perfluoro side chains, containing sulfonic acid groups as the
264 functional groups [26]. For the fresh membrane, the thermal degradation reaches its
265 maximum rate at 500 °C (attributed to the sum of a series–parallel degradation
266 reactions of both the polymer and the functional group [27]) as evidenced by the
267 peak in the TGA profile (Fig. 3C). This peak gets displaced towards lower
268 temperatures (460 °C) after the first month, probably as a result of the loss of the
269 protective layer. The TGA profiles get unaltered in the samples taken in the following
270 months, thus showing a remarkable chemical and thermal stability similarly to that
271 observed in the CMI-7000.

272 The FKB and FKE are both based on perfluorinated sulfonic acid and are
273 manufactured by the same company (Fumatech) [28]. For both, the fresh
274 membranes present two transitions of mass loss at around 230 and 320 °C, which
275 are attributed to stabilizing agents and another wider one, between 400 and 600 °C,
276 which is attributed to the degradation of sulfonated polyether ketones. After the first
277 month of use, the first peak at 320 °C almost disappears in both membranes
278 (because of the removal of the stabilizing agents) and the second peak (at 550 °C)
279 moves to lower temperatures, showing a degradation pattern similar to that of the
280 Zirfon.

281 Overall, these results show that Nafion and CMI-7000 have an excellent thermal
282 stability in long-term operation, in contrast to Zirfon, FKB and FKE that follow a
283 moderate degradation pattern along time.

284 3.3. Assessment of electrochemical properties through IEC

285 The ion exchange capacity (IEC) is the number of fixed charges inside the cation
286 exchange membrane per unit of weight of the dry polymer. The importance of this
287 parameter lays in the fact that IEC is indirectly linked to the proton conductivity of the
288 polymer [29,30] and thus it affects other important membrane properties such as its
289 electrical resistance [31]. Figure 5 illustrates the evolution of the IEC values along
290 the four months of operation. It shows that IEC did not changed substantially for any
291 of them, except for the FKE, where a clear drop appears between the third and the
292 fourth month of operation with a descent of 18% (although it still kept the highest IEC
293 value). The Nafion membrane underwent a similar reduction (20%), but in this case it
294 was a more gradual one.



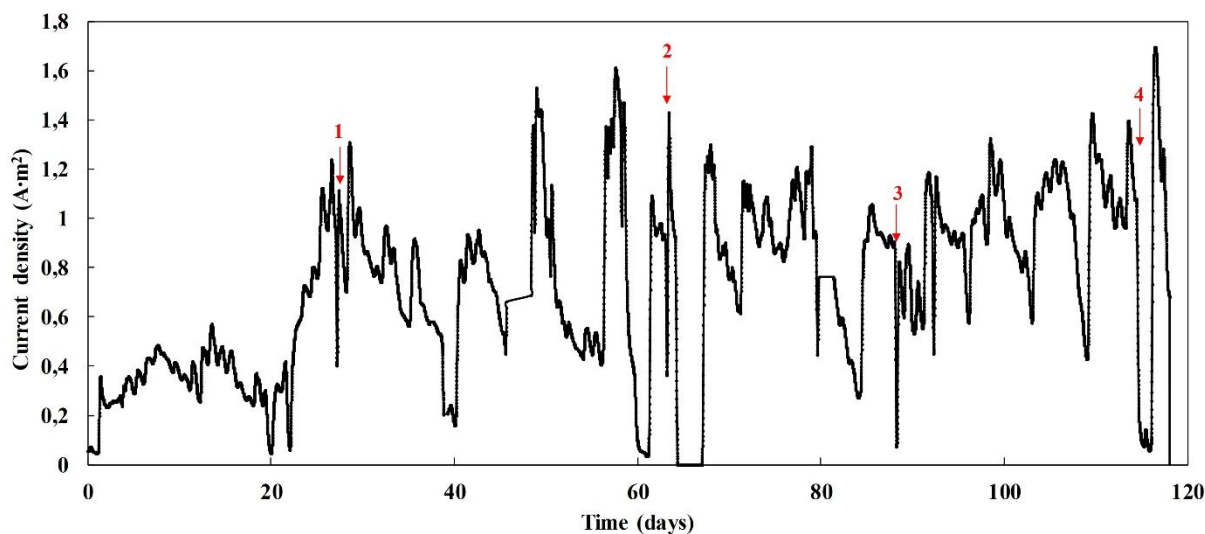
296

297 **Figure 5.** Evolution of Ion Exchange Capacity (meq/g) along operation time.

298 3.4. MEC performance and final comments

299 Cation exchange membranes play a key role on both the economic feasibility
 300 and on the electrochemical performance of BES. Assessing their long-term stability
 301 becomes, thus, a key issue in process design and cost calculation [32]. Overall, our
 302 results show that, at least from the ageing perspective, there is not an ideal cation
 303 exchange membrane (among those commercially available) for BES. For instance,
 304 the chemical structure of membranes such as FKE, that are less prone to fouling and
 305 biofouling (on account of their resilience to surface deterioration) and that score the
 306 highest IEC, seem to degrade more rapidly as revealed by the thermal analysis. In
 307 contrast, CMI-7000 and even Nafion, which display a remarkable thermal stability
 308 after the first month of operation (initial degradation can be attributed to the loss of
 309 the protective layer) show a rapid increase of surface roughness and therefore of
 310 fouling.

311



312

313 **Figure 6.** Current density profile over the 120 days periods of operation (Arrows indicate
 314 membrane sampling at 1, 2, 3 and 4 months).

315

316 Here, it is important to bring to mind that the membranes investigated in this study
 317 are typically used in conventional electrochemical systems where current densities
 318 can be as high as $10,000 \text{ A}\cdot\text{m}^{-2}$ [33]. This contrasts with the $\sim 1 \text{ A}\cdot\text{m}^{-2}$ (Figure 6)
 319 measured in our cell, which is an usual current density for BES [34] but highlights
 320 the low electrical stress to which conventional membranes are subjected in BES
 321 applications. In other words, existing commercial membranes are somehow
 322 “oversized” when used in BES. This, of course, would not be a problem if it were not for
 323 the relatively large cost that these membranes have (Table 1). The challenge is thus
 324 to develop “tailor-made” membranes, that can show a fair long-term stability and
 325 resilience, with an economic cost that does not threaten the commercial development of
 326 BES. In this regard, new developments that can provide similar or even better results
 327 than commercial membranes at a cheaper cost are already underway [24]. These
 328 advances are also helping to expand the range of applications of BES [35,36],
 329 opening new exciting possibilities and paving their way towards practical
 330 applicability.

331 **4. Conclusions**

332 The ion exchange membrane explains much of the cost of BES and its durability
 333 has a marked impact on their economic feasibility. In this study, we compared the
 334 ageing process of 5 commercially available cation exchange membranes. Nafion

335 and CMI-7000 showed a remarkably robust chemical structure, although they suffer
336 the greatest surface modification. This revealed a tendency to promote fouling and
337 biofouling that was more pronounced than in FKB and, specially, than in FKE. The
338 ion exchange capacity, which is related to the electric conductivity of the
339 membranes, showed a moderate decay in all membranes. Despite these apparent
340 signs of deterioration, the current density kept almost constant ($\sim 1 \text{ A m}^{-2}$) which
341 suggest that the studied membranes can maintain their electrochemical
342 performance within the demanding environment of BES.

343

344 **Acknowledgments**

345 This research was possible thanks to the financial support of the 'Ministerio de
346 Economía y Competitividad' (ref: CTQ2015-68925-R), project cofinanced by FEDER
347 funds. M.I. San-Martín is supported by an FPU fellowship grant (FPU13/04014) from
348 the Spanish Ministry of Economy and Competitiveness.

349

350

351 **References**

- 352 [1] Zhang S, Bao R, Lu J, Sang W. Simultaneous sulfide removal, nitrification, denitrification and
353 electricity generation in three-chamber microbial fuel cells. *Sep Purif Technol*
354 2018;195:314–21. doi:10.1016/J.SEPPUR.2017.12.027.
- 355 [2] Li S, Chen G, Anandhi A. Applications of Emerging Bioelectrochemical Technologies in
356 Agricultural Systems: A Current Review. *Energies* 2018;11. doi:10.3390/en11112951.
- 357 [3] San-Martín MI. Bioelectrochemical Systems for Energy Valorization of Waste Streams. In:
358 Leicester DD, editor., Rijeka: IntechOpen; 2018, p. Ch. 8. doi:10.5772/intechopen.74039.
- 359 [4] Escapa A, Mateos R, Martínez EJ, Blanes J. Microbial electrolysis cells: An emerging
360 technology for wastewater treatment and energy recovery. From laboratory to pilot plant and
361 beyond. *Renew Sustain Energy Rev* 2016;55:942–56. doi:10.1016/j.rser.2015.11.029.
- 362 [5] Sleutels THJA, ter Heijne A, Kuntke P, Buisman CJN, Hamelers HVM. Membrane Selectivity
363 Determines Energetic Losses for Ion Transport in Bioelectrochemical Systems.
364 *ChemistrySelect* n.d.;2:3462–70. doi:10.1002/slct.201700064.
- 365 [6] Leong JX, Daud WRW, Ghasemi M, Liew K Ben, Ismail M. Ion exchange membranes as
366 separators in microbial fuel cells for bioenergy conversion: A comprehensive review. *Renew*
367 *Sustain Energy Rev* 2013;28:575–87. doi:10.1016/J.RSER.2013.08.052.
- 368 [7] Ceconet D, Callegari A, Capodaglio GA. Bioelectrochemical Systems for Removal of
369 Selected Metals and Perchlorate from Groundwater: A Review. *Energies* 2018;11.
370 doi:10.3390/en11102643.
- 371 [8] Tartakovsky B, Kleiner Y, Manuel M. Bioelectrochemical anaerobic sewage treatment
372 technology for Arctic communities. *Environ Sci Pollut Res* 2017:0–6.
373 doi:10.1007/s11356-017-8390-1.
- 374 [9] Yan T, Ye Y, Ma H, Zhang Y, Guo W, Du B, et al. A critical review on membrane hybrid system
375 for nutrient recovery from wastewater. *Chem Eng J* 2018;348:143–56.
376 doi:10.1016/J.CEJ.2018.04.166.
- 377 [10] San-Martin MI, Leicester DD, Heidrich ES, Alonso RM, Mateos R, Escapa A.
378 Bioelectrochemical Systems for Energy Valorization of Waste Streams. *Energy Syst. Environ.*,
379 IntechOpen; 2018.

- 380 [11] Hernández-Flores G, Poggi-Varaldo HM, Solorza-Feria O. Comparison of alternative
381 membranes to replace high cost Nafion ones in microbial fuel cells. *Int J Hydrogen Energy*
382 2016;41:23354–62. doi:10.1016/J.IJHYDENE.2016.08.206.
- 383 [12] Yuan H, He Z. Integrating membrane filtration into bioelectrochemical systems as next
384 generation energy-efficient wastewater treatment technologies for water reclamation: A
385 review. *Bioresour Technol* 2015;195:202–9. doi:10.1016/J.BIORTECH.2015.05.058.
- 386 [13] Chacón-Carrera RA, López-Ortiz A, Collins-Martínez V, Meléndez-Zaragoza MJ,
387 Salinas-Gutiérrez J, Espinoza-Hicks JC, et al. Assessment of two ionic exchange membranes
388 in a bioelectrochemical system for wastewater treatment and hydrogen production. *Int J*
389 *Hydrogen Energy* 2018. doi:10.1016/J.IJHYDENE.2018.10.153.
- 390 [14] Hernández-Fernández FJ, de los Ríos AP, Mateo-Ramírez F, Juárez MD, Lozano-Blanco LJ,
391 Godínez C. New application of polymer inclusion membrane based on ionic liquids as proton
392 exchange membrane in microbial fuel cell. *Sep Purif Technol* 2016;160:51–8.
393 doi:10.1016/J.SEPPUR.2015.12.047.
- 394 [15] Li W-W, Sheng G-P, Liu X-W, Yu H-Q. Recent advances in the separators for microbial fuel
395 cells. *Bioresour Technol* 2011;102:244–52. doi:10.1016/J.BIORTECH.2010.03.090.
- 396 [16] San-Martín MI, Sotres A, Alonso RM, Díaz-Marcos J, Morán A, Escapa A. Assessing anodic
397 microbial populations and membrane ageing in a pilot microbial electrolysis cell. *Int J*
398 *Hydrogen Energy* 2019. doi:10.1016/J.IJHYDENE.2019.01.287.
- 399 [17] Mateos R, Alonso RM, Escapa A, Morán A. Methodology for Fast and Facile Characterisation
400 of Carbon-Based Electrodes Focused on Bioelectrochemical Systems Development and
401 Scale Up. *Materials (Basel)* 2017;10.
- 402 [18] del Pilar Anzola Rojas M, Mateos R, Sotres A, Zaiat M, Gonzalez ER, Escapa A, et al.
403 Microbial electrosynthesis (MES) from CO₂ is resilient to fluctuations in renewable energy
404 supply. *Energy Convers Manag* 2018;177:272–9. doi:10.1016/J.ENCONMAN.2018.09.064.
- 405 [19] Silva V, Montalvillo M, Carmona FJ, Palacio L, Hernández A, Prádanos P. Prediction of single
406 salt rejection in nanofiltration membranes by independent measurements. *Desalination*
407 2016;382:1–12. doi:10.1016/J.DESAL.2015.12.012.
- 408 [20] Johnson D, Hilal N. Characterisation and quantification of membrane surface properties using

- 409 atomic force microscopy: A comprehensive review. *Desalination* 2015;356:149–64.
410 doi:10.1016/j.desal.2014.08.019.
- 411 [21] Xu J, Sheng G-P, Luo H-W, Li W-W, Wang L-F, Yu H-Q. Fouling of proton exchange
412 membrane (PEM) deteriorates the performance of microbial fuel cell. *Water Res*
413 2012;46:1817–24. doi:10.1016/J.WATRES.2011.12.060.
- 414 [22] Flimban SGA, Hassan SHA, Rahman MM, Oh S-E. The effect of Nafion membrane fouling on
415 the power generation of a microbial fuel cell. *Int J Hydrogen Energy* 2018.
416 doi:10.1016/J.IJHYDENE.2018.02.097.
- 417 [23] Meng F, Liao B, Liang S, Yang F, Zhang H, Song L. Morphological visualization, componential
418 characterization and microbiological identification of membrane fouling in membrane
419 bioreactors (MBRs). *J Memb Sci* 2010;361:1–14. doi:10.1016/J.MEMSCI.2010.06.006.
- 420 [24] Zinadini S, Zinatizadeh AA, Rahimi M, Vatanpour V, Rahimi Z. High power generation and
421 COD removal in a microbial fuel cell operated by a novel sulfonated PES/PES blend proton
422 exchange membrane. *Energy* 2017;125:427–38. doi:10.1016/J.ENERGY.2017.02.146.
- 423 [25] CMI-7000 Cation Exchange Membranes: Membranes International Inc. n.d.
424 [https://membranesinternational.com/cmi-7000-cation-exchange-membranes-technical-specifi](https://membranesinternational.com/cmi-7000-cation-exchange-membranes-technical-specifications)
425 [cations](https://membranesinternational.com/cmi-7000-cation-exchange-membranes-technical-specifications)
- 426 [26] ZIRFON PERL UTP 500 - Specialty Products n.d.
427 <http://www.agfa.com/specialty-products/solutions/membranes/zirfon-perl-utp-500/>
- 428 [27] Deng Q, Wilkie CA, Moore RB, Mauritz KA. TGA–FTi.r. investigation of the thermal
429 degradation of Nafion® and Nafion®/[silicon oxide]-based nanocomposites. *Polymer (Guildf)*
430 1998;39:5961–72. doi:10.1016/S0032-3861(98)00055-X.
- 431 [28] Products - fumatech GmbH n.d.
432 <https://www.fumatech.com/EN/Membranes/Water+treatment/Products+fumasep/>
- 433 [29] Navessin T, Holdcroft S, Wang Q, Song D, Liu Z, Eikerling M, et al. The role of membrane ion
434 exchange capacity on membrane|gas diffusion electrode interfaces: a half-fuel cell
435 electrochemical study. *J Electroanal Chem* 2004;567:111–22.
436 doi:10.1016/J.JELECHEM.2003.12.042.
- 437 [30] Chuy C, Basura VI, Simon E, Holdcroft S, Horsfall J, Lovell K V. Electrochemical

438 Characterization of Ethylenetetrafluoroethylene-g-polystyrenesulfonic Acid Solid Polymer
439 Electrolytes. *J Electrochem Soc* 2000;147:4453–8.

440 [31] Wilhelm FG, Pünt IGM, van der Vegt NFA, Strathmann H, Wessling M. Cation permeable
441 membranes from blends of sulfonated poly(ether ether ketone) and poly(ether sulfone). *J*
442 *Memb Sci* 2002;199:167–76. doi:[https://doi.org/10.1016/S0376-7388\(01\)00695-0](https://doi.org/10.1016/S0376-7388(01)00695-0).

443 [32] Giorno L, Drioli E, Strathmann H. Ion-Exchange Membrane Characterization BT -
444 *Encyclopedia of Membranes*. In: Drioli E, Giorno L, editors., Berlin, Heidelberg: Springer Berlin
445 Heidelberg; 2016, p. 1052–6. doi:10.1007/978-3-662-44324-8_994.

446 [33] Peighambaroust SJ, Rowshanzamir S, Amjadi M. Review of the proton exchange
447 membranes for fuel cell applications. *Int J Hydrogen Energy* 2010;35:9349–84.
448 doi:10.1016/J.IJHYDENE.2010.05.017.

449 [34] Rahimnejad M, Adhami A, Darvari S, Zirepour A, Oh S-E. Microbial fuel cell as new
450 technology for bioelectricity generation: A review. *Alexandria Eng J* 2015;54:745–56.
451 doi:10.1016/J.AEJ.2015.03.031.

452 [35] Kuntke P, Zamora P, Saakes M, Buisman CJN, Hamelers HVM. Gas-permeable hydrophobic
453 tubular membranes for ammonia recovery in bio-electrochemical systems. *Environ Sci Water*
454 *Res Technol* 2016;2:261–5. doi:10.1039/c5ew00299k.

455 [36] Yuan H, He Z. Integrating membrane filtration into bioelectrochemical systems as next
456 generation energy-efficient wastewater treatment technologies for water reclamation: A
457 review. *Bioresour Technol* 2015;195:202–9. doi:10.1016/J.BIORTECH.2015.05.058.

458

459

Figure 1
[Click here to download high resolution image](#)

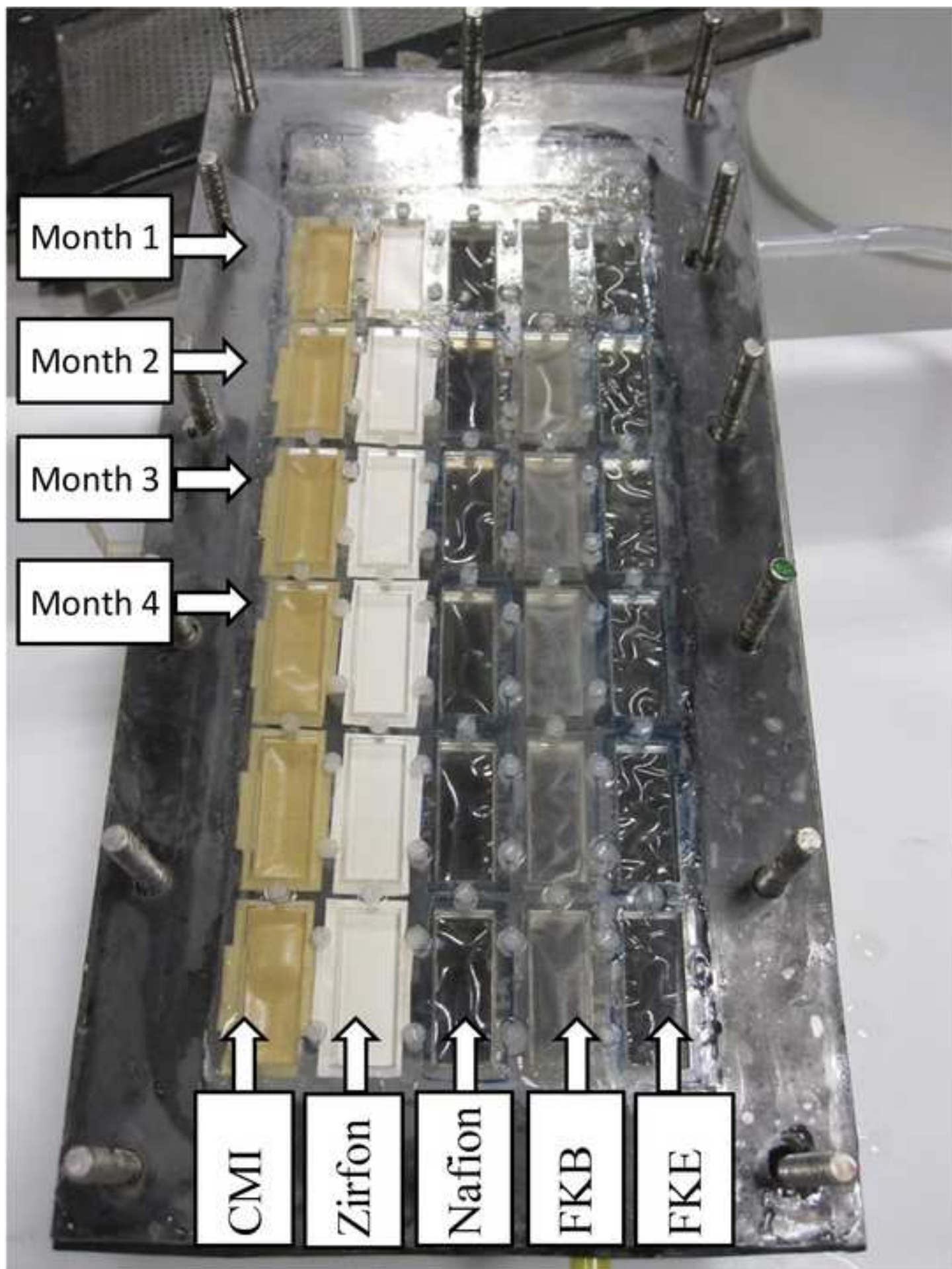


Figure 2
[Click here to download high resolution image](#)

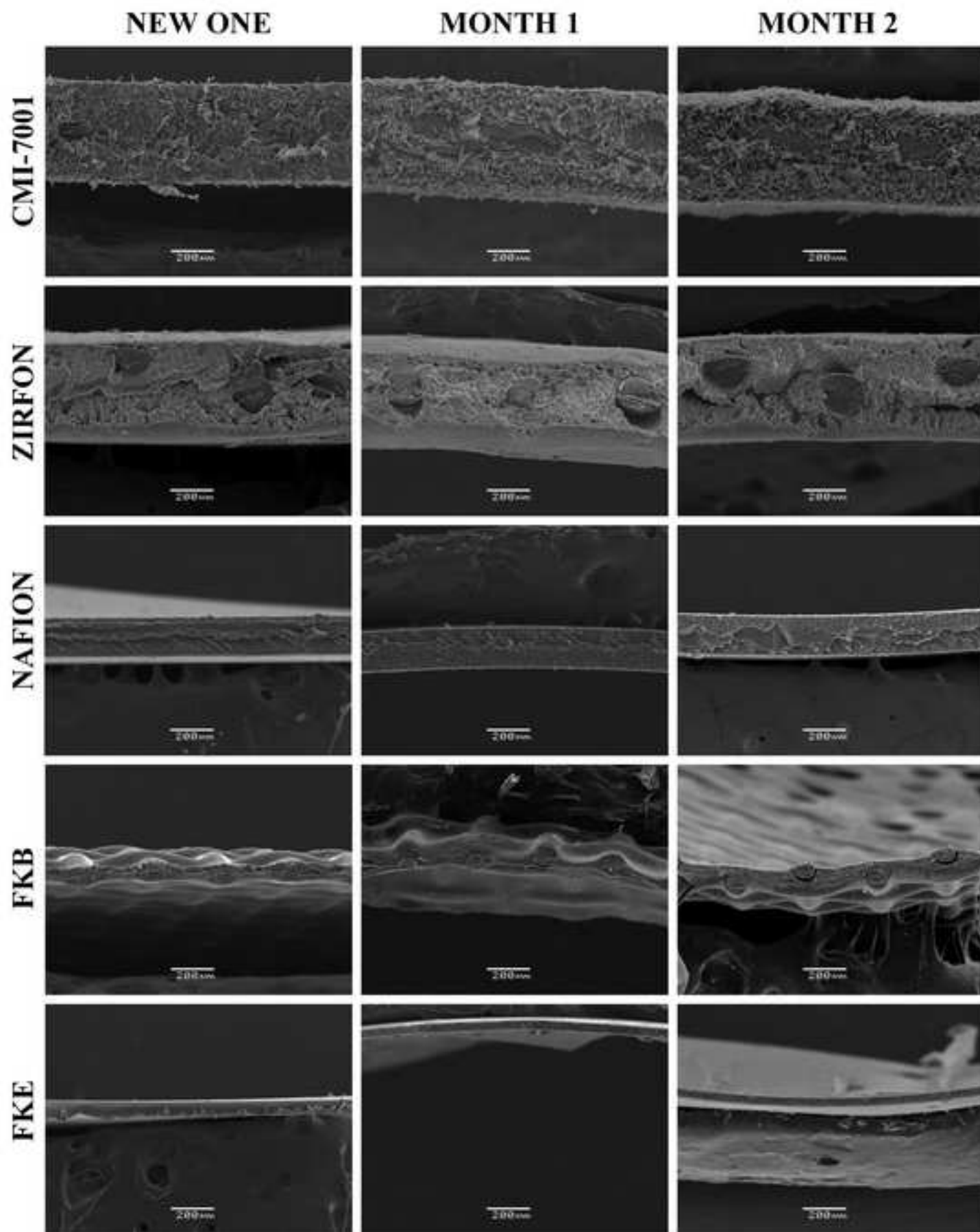


Figure 3
[Click here to download high resolution image](#)

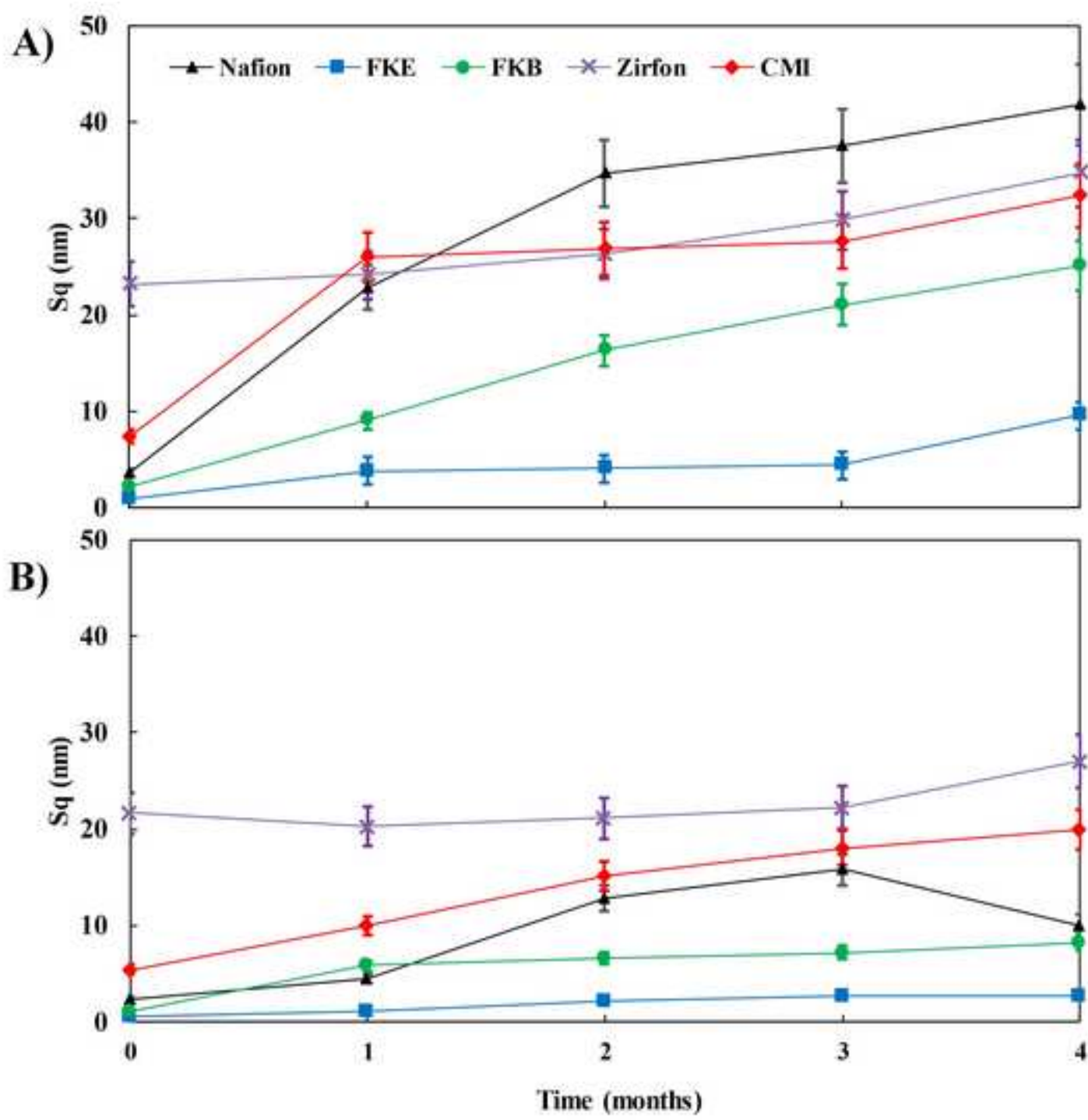


Figure 4

[Click here to download high resolution image](#)

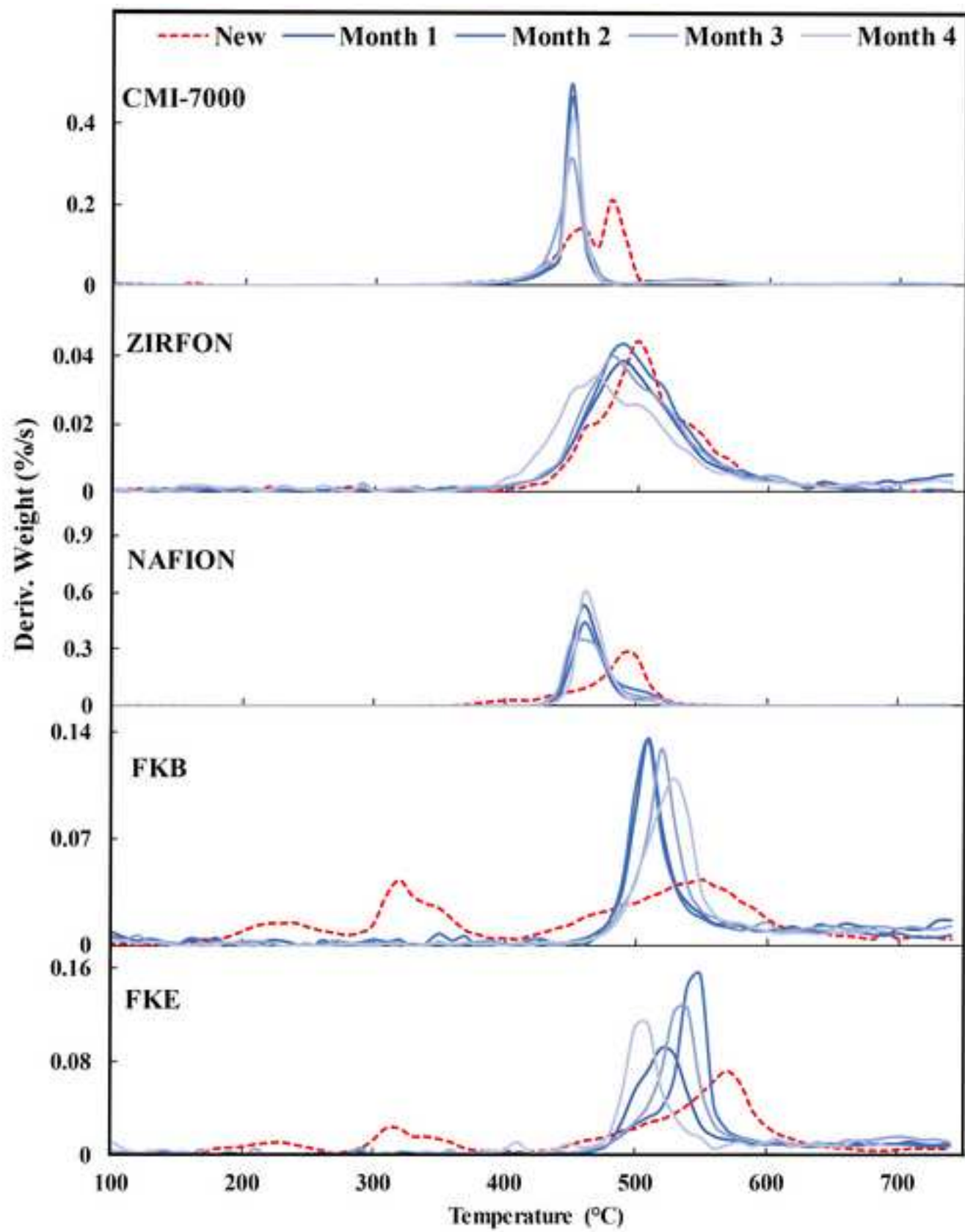


Figure 5
[Click here to download high resolution image](#)

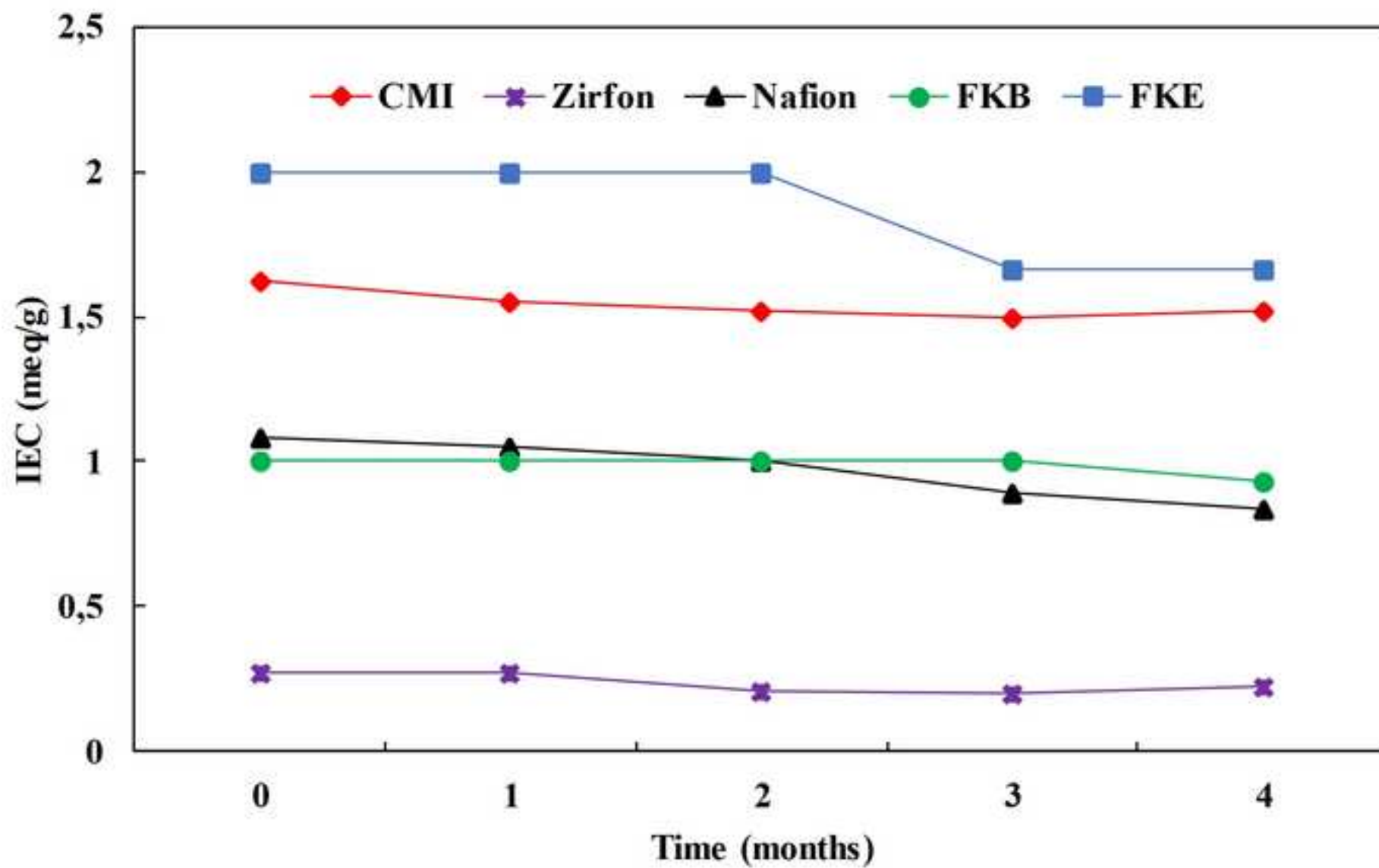


Figure 6
[Click here to download high resolution image](#)

